

Influence of Xyloglucan Molar Mass on Rheological Properties of Cellulose Nanocrystal/Xyloglucan Hydrogels

Malika Talantikite^{1,*}, Antoine Gourlay¹, Sophie Le Gall¹ and Bernard Cathala¹

¹UR1268 Biopolymères Interactions Assemblages, INRA, 44316, Nantes, France.

*Corresponding Author: Malika Talantikite. Email: malika.talantikite@inra.fr.

Abstract: Plant components are an inexhaustible source for the construction of bio-based materials. Here we report, for the first time, the elaboration of biobased cellulose nanocrystals (CNC)/xyloglucan (XG) hydrogels. XG is a hemicellulose displaying a great affinity for cellulose surface and can be thus irreversibly adsorbed on CNC. Properties of the hydrogels were investigated by varying the molar mass of XG either by enzymatic treatment with Endo-glucanase (EG2) or physical fractionation by ultrasound (US). Fractions were characterised by high-performance size exclusion chromatography (HPSEC) and their monosaccharide decompositions were determined. Three fractions with high, average and small molar mass, (800, 300 and 100 10³ g/mol respectively), were selected in order to tune the properties of the hydrogel. Sol-gel transition conditions were determined for each fraction by achieving phase diagram using the inverted tube method. Mechanical properties, assessed by rheology, are improved by increasing XG molar mass since elastic modulus is higher for hydrogels formed with higher molar mass fractions as well as the strain at break. Gel formation is likely due to the adsorption of XG fractions on CNC which increases the effective hydrodynamic volume of CNC leading to steric stabilization and interactions between loops and tails of XG adsorbed.

Keywords: Cellulose nanocrystals; xyloglucan fractions; rheology; hydrogels

1 Introduction

Cellulose is one of the most abundant renewable resources on Earth. Since several decades, disruption of cellulose fibers down to nanoscale opened tremendous opportunities to generate amazing materials referred as nanocellulose. Among nanocelluloses, cellulose nanocrystals (CNC) are stiff nanorods obtained by harsh acid hydrolysis. Thanks to their colloidal properties, high specific surfaces and surface chemistry, CNCs have been the subject of intense research to design innovative biobased materials among which composites, emulsions, foams and hydrogels [1-4].

Xyloglucans (XG) are an hemicellulose family identified as key component of the primary cell walls of growing plant [5]. XG has a cellulose-like backbone composed of 1, 4-linked, β -glucopyranosyl residues. This backbone consists typically in blocks of four successive glucose units among which three of them carry a flexible α -(1, 6) linked D-xylosyldecoration, either as a single sugar or as a β -D-Gal-(1, 2)- α -D-Xyl/ or α -l-Fuc-(1, 2)- β -D-Gal-(1, 2)- α -D-Xyl side chains, however a wide variability has been identified among plants [5,6]. Even if the complete scheme of cellulose/XG interactions and their role in plant cell are still a matter of debate, XG and cellulose interact intimately *in vivo* with cellulose via hydrogen bonds, van der Waals interactions, and polar interactions [7,8-10,11-14]. XG adsorption behaviour has been reported to be entropically and kinetically driven and thus molar mass of XG is a key point for the deeper understanding of the final properties of the assemblies. *In vitro* experiments have also highlighted the strong interactions that exist between cellulose with different surface morphologies and XG from different sources with different molar masses, different structures and at different ratios [15-17]. XG adsorption on CNC has been studied

as model investigation for hemicellulose/cellulose interactions but also as a versatile process for biobased materials elaboration [18]. Amount of XG adsorbed vary quantitatively and qualitatively depending on CNC-XG ratio, since it was reported that at low CNC-XG ratio the whole chain of XG is bounded to CNC in contrast at high CNC-XG ratio XG forms tails and loops on the surface of CNC [17-19]. XG molar mass has a huge impact on CNC-XG association, it was demonstrated that even if both high and low XG molar mass strongly adsorb irreversibly on CNC surfaces, low XG molar mass polymers form extended layers that coat CNC whereas XG with high molar mass forms loops and tails on CNC surface [17,20]. It was also shown that XG regardless its molar mass is able to cross link cellulose nanocrystals in layer by layer CNC-XG-CNC assemblies [17,21,22]. In addition it was also reported that galactose substitution of XG is a major determinant of cellulose composite and properties [20]. Accordingly, variation of the XG structure is a key point to tune biobased materials properties based on XG as well as a relevant strategy to understand cell wall architecture.

Hydrogels as their name suggests are gels containing a large amount of water trapped in a three-dimensional network of hydro soluble polymers. This high water content makes them good candidates for construction of materials for applications in biomedical field [23]. They already found uses on cosmetics and also have variety of applications such as in chromatography, food and also in domestic uses [24]. Cellulose based hydrogels have been already reported thanks to their high strength, large specific surface, and tunable surface chemistry, allowing controlled interactions with various building blocks to achieve materials with tunable and efficient properties [3,25]. CNC based hydrogels can be implemented through chemical or physical pathway among which polymer addition has been reported as efficient strategy [26,27]. Nevertheless, fully biobased CNC hydrogels are still seldom and to our knowledge, CNC/XG hydrogels have never been reported.

In this work, we explore the effect of XG molar mass on formation of hydrogels composed of XG and CNC. Such hydrogels have never been reported before to the best of our knowledge. We used different XG fractions obtained by ultra-sonication and enzymatic treatment. Fraction molar masses were determined by high-performance size exclusion chromatography (HPSEC) and their composition was investigated by monosaccharide analysis. Three fractions with contrasted molar masses but identical monomeric composition was selected to implement phase diagrams. Depending on XG molar masses, gel formation occurs at different CNC/XG concentration ratio. Rheological tests were used to measure the mechanical properties of the gels and their ability to reform after breaking was assessed.

2 Experimental Section

CNC were purchased from CelluForce (Canada), they were obtained by acid hydrolysis of wood pulp and according to product specification (Crystalline fraction = 0.88 (by XRD), surface charge density = 0.023 mmol/g (by conductivity), pH (dispersed in water) = 6-7, crystallite diameter = 2.3-4.5 nm (by AFM), crystallite length = 44-108 nm (by AFM)) CNC solutions were prepared by dispersing CNC in milli-Q water. Dispersion was vigorously stirred during 24 h and finally sonicated. Tamarind seed gum XG (XG-C) was purchased from DSP GOYKO FOOD&CHEMICAL (Japan). Xyloglucan was used after precipitation in ethanol. XG solution was stirred during a night. Endo-Cellulase EG2 enzyme (EC 3.2.1.4) was purchased from Megazyme (Ireland).

2.1 Preparation of Different Fractions of Xyloglucan

2.1.1 Endoglucanase Treatment

XG solution at 14.7 g/L was prepared in 600 mL of acetate buffer pH = 4.5. Solution was heated at 30°C and endoglucanase was added at 1 mU/mg of XG from a stock solution at 700 U/mL. Reaction times were 30, 60, 240 min for samples that were named respectively E-30, E-60, E-240. Reaction was stopped by adding few droplets of ammonia at 25% (Fluka Chemika). Samples were precipitated twice into 1.2 L of EtOH 96% (Carlo Erba Reagenti SPA) and vacuum filtered. The precipitates were finally washed with diethyloxide 99.5% (QP Panreac), vacuum filtered and dried under fume cupboard.

2.1.2 Ultra-sonication Treatment

200 mL XG solutions at 10 g/L were sonicated using Sonicator Qsonica (Q700; 230 V; 700 W; 20 kHz) with a microtip 1/2", 25% of amplitude and 2/2 on/off sonication for 5 min steps with stirring between each step to homogenize the ultra-sonication through the sample. Three samples were prepared at different times of sonication (10 min, 20 min and 40 min) samples were named respectively US-10, US-20, US-40. Final XG fractions were obtained after dialysis and freeze-drying.

2.2 High-Performance Size-Exclusion Chromatography (HPSEC)

XG fractions were dissolved at 5 g/L in 50 mM NaNO₃ (99% Sigma Ultra S8170-250G) and filtrated at 0.1 μm before measurement. Eluent consists in 50 mM NaNO₃ containing 0.02% NaN₃ and filtrated at 0.1 μm. The samples were eluted at 0.6 mL/min. The column used was Shodex OHpak SB-805 HQ column (8 mm × 300 mm). On-line molar mass and intrinsic viscosity determinations were performed using a multi-angle laser light scattering (MALLS) detector (mini-Dawn, Wyatt, USA), a differential refractometer (ERC 7517 A) and a differential viscometer (T-50A, Viscotek, USA) [28]. Molar masses were determined using ASTRA 1.4 software (Wyatt, USA). The concentrations were calculated using a $dn/dc = 0.147$ mL/g.

2.3 Monosaccharides Analysis

Identification and quantification of neutral sugars were performed by gas-liquid chromatography after sulfuric acid degradation. Briefly, 5 mg of each sample were dispersed in 13 mol/L sulfuric acid for 30 min at 30°C and then hydrolyzed in 1 mol/L sulfuric acid (2 h, 100°C). Sugars were converted to alditol acetates according to [29] and chromatographed on a TG-225 GC Column (30 × 0.32 mm ID) using TRACE™ Ultra Gas Chromatograph (Thermo Scientific™; temperature 205°C, carrier gas H₂). Standard sugars solution and inositol as internal standard were used for quantification.

2.4 Phase Diagram

XG solutions were prepared by dissolving the XG into pure water. Various mixtures were then prepared by varying the concentration of XG (0.1 to 20 g/L) and CNC (1 to 15 g/L) (final volume 3 mL). Then, a reverse tube test was performed for each sample by turning the tube upside down to submit it to its own weigh. Gelation was visually determined by assessing if the XG/CNC mixtures flow or not.

2.5 Rheology

Rheological measurements were performed using stress-controlled rheometer AR-2000 (TA Instruments) equipped with truncated cone (40 mm diameter, 2° cone). Samples were covered with paraffin oil to prevent drying. Measurements were made on the linear domain.

3 Results

3.1 Characterisation of the XG Fractions

XG molar fractionation was achieved by using ultrasound (referenced as US) or enzymatic treatment (referenced as E). These two methods lead to the decrease of the molar mass of the XG by increasing time of treatment allowing the access to a broad panel of polymers (Tab. 1). M_w of the starting sample is in the range of 800×10^3 gmol⁻¹ while the lowest molar mass was obtained after 240 min of enzymatic treatment and is in the range of 100×10^3 gmol⁻¹. The reduction of molecular size is also demonstrated by the viscometric hydrodynamic radii that decrease from 44 nm to 11 nm as well as intrinsic viscosity: 716 mL/g to 123 mL/g for XGC and XGE 240 respectively. Gyration radii were also determined; it decreases from 72 nm down to less than 30-20 nm. Indeed, R_g cannot be calculated for the lowest molar masses from the MALLS data since they display no angular dependency.

Table 1: Macromolecular characteristics of XG fractions analyzed by HPSEC-MALLS-VS-RI. M_w : molar mass average in weight; M_n : molar mass average in number; M_w/M_n : polydispersity index; R_g : gyration radius; R_h : hydrodynamic radius; $[\eta]$: intrinsic viscosity

	M_w (10^3 g mol^{-1})	M_w/M_n	R_g (nm)	R_h (nm)	$[\eta]$ mL g $^{-1}$
XG C	840	1.24	72	44	716
E 30	334	1.57	33	25	366
E 60	189	1.62	-	18	235
E 240	85	1.72	-	11	123
US 10	584	1.33	55	33	567
US 20	436	1.39	43	31	472
US 40	326	1.52	32	25	315

The use of a combined SEC-MALLS analysis made possible to plot the average molar mass (M_w) distribution as a function of the radii of gyration (R_g) (Fig. 1(a)). The slope of this plot provides valuable information regarding the conformational changes and it was found that for all the molar masses of the fractions or the method of cleavage (E or US), all the points are aligned. This indicates that all the fractions display similar conformation. The value of the slope gives some insight about the conformation behaviors. A slope of 0.33 indicates a sphere; a slope of 0.5-0.6 shows a random coil while a slope of 1 indicates a rod-shape structure. The value of the slope obtained for the XG fractions (Fig. 1(a)) is about of 0.6 indicating that all the fractions has a random coil conformation. The Mark-Houwink equation $[\eta] = K \cdot M_w^a$ has been also established and lead to similar conclusion (Fig. 2(a)). The slope value of the linear fit the $\log([\eta])$ vs $\log(M_w)$ is equal to 0.79 and is characteristic of a random coil conformation. Similar values have already been measured for other semi-flexible hemicelluloses such as arbinoxylans [28] and galactomannan [30]. Thus it can be concluded from these results that the molar mass fractionation do not change the conformational behaviours of the XG fractions.

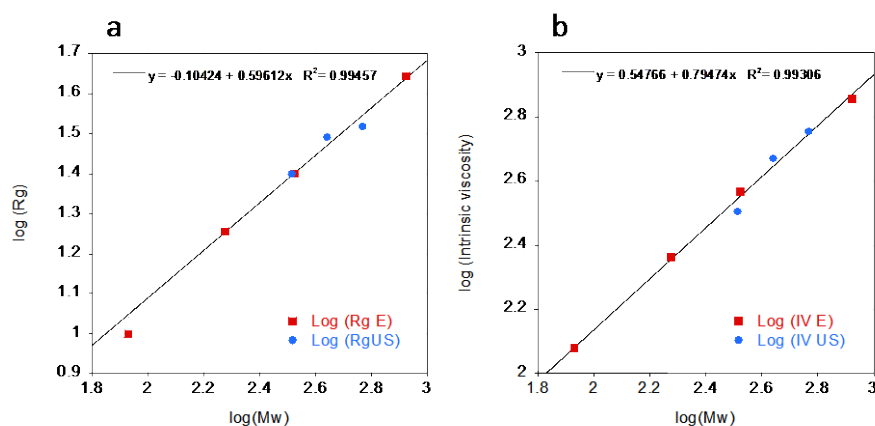


Figure 1: A plot of $\log(R_g)$ against $\log(M_w)$ for XG fractions obtained by enzymatic (E) (red square) and ultra-sound (US) (blue point); b Plot of $\log(\text{intrinsic viscosity, IV})$ against $\log(M_w)$: Mark-Houwink relationship for XG fractions obtained by enzymatic (red square) and ultra-sound (blue point)

We also investigated the monosaccharide composition of the fractions. Monosaccharides analysis of the different fractions (Fig. 2) shows that the XG fractions have the same composition of saccharide. They display the expected composition for Tamarind XG, i.e., namely c.a. 50% of Glucose; 30% of Xylose; about 15-17% of Galactose and some traces of arabinose. From all these results we can conclude that both

enzymatic and ultra-sound treatment do not affect neither the conformation of the polymers or their chemical structure.

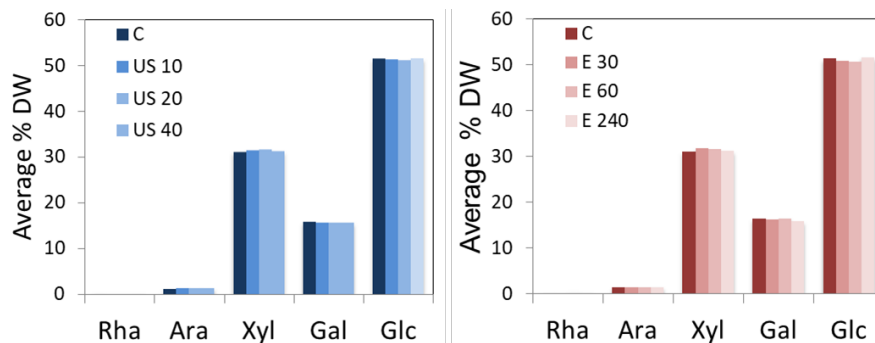


Figure 2: Monosaccharide composition of fractions of XG prepared with enzymatic treatment (E) with Endoglucanase and with ultra-sonication (US)

The rest of our study will be focused on three fractions that cover the range of molar mass obtained. We selected the starting XG sample that has a molar mass of $840 \cdot 10^3$ g/mol, a fraction with an intermediate value, i.e., US 40 that has a molar mass of $326 \cdot 10^3$ g/mol and the lowest molar mass fraction, i.e., E 240 ($85 \cdot 10^3$ g/mol). For clarity reasons, the fractions will be referred as XG 800, XG 300 and XG 100 according to their molar mass values in the following sections. The choice of these fractions with contrasted molar mass is motivated the different adsorption behaviour of XG fractions with different molar on CNC surfaces that we previously reported [17]. We demonstrated that adsorption conformation of XG change according to the molar mass. We thus expect a variation of XG/CNC complexes architecture that will impact the gelling behaviour and thus a will offer a tool for tuning the properties of the aerogels.

3.2 Phase Diagram

The aim of this work is to investigate the formation of hydrogel composed of XG and CNC and more specifically the influence of the XG molar mass on the properties of the gel. Thus the first step is to determine the concentration ratio at which gels are formed. This was achieved by the implementation of phase diagrams obtained by preparing mixtures containing different ratio concentrations of CNC and XG fractions (XG 800; XG 300; XG 100) (Fig. 3). Determination of solution states was carried out by the inverted tube method which consists in mixing of XG and CNC and turning the tube upside down. Solutions appeared on three different states: liquids that flow immediately, viscous liquids that flow very slowly and gels that did not flow upon their own weight. We observed that invertible gels are formed with the highest molar mass XG fractions, XG 800 and XG 300. To our knowledge, our work is the first report of CNC/XG hydrogels. In the case of XG 100, only viscous liquids are obtained. In the case of XG 800 and XG 300, hydrogels were obtained for the same XG concentration (5 g/L) but for different CNC concentration 5 and 15 g/L for XG 800 and XG 300 respectively. It has to be note that in all the cases, no phase separation was observed suggesting a good dispersion of CNC/XG complexes.

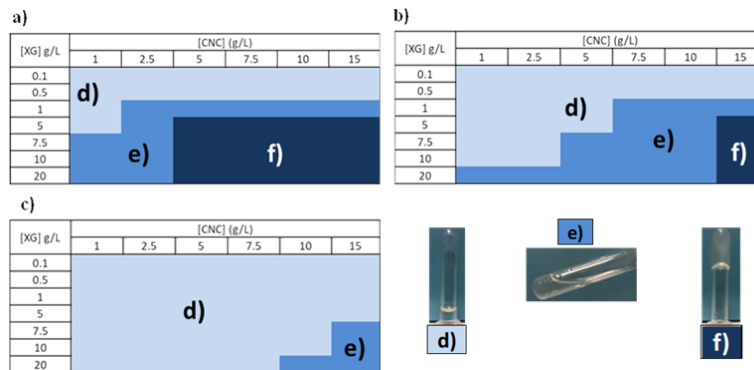


Figure 3: Phase diagram of mixtures containing CNC and XG fractions at a) XG 800, b) XG 300 and c) XG 100, mixtures are on three different states: d) liquid, e) viscous liquid and e) gel, at 20°C

3.3 Rheological Measurements

Dynamic mechanical properties were investigated by measuring the frequency dependence of the elastic (G') and viscous (G'') moduli. XG molar mass effect on mechanical properties of solutions containing 10 g/L CNC was investigated (Fig. 4(a)). In case of low molar mass XG fraction (XG 100) solution behaves like a viscoelastic liquid, elastic (G') and viscous (G'') moduli are very low and almost superimposed. A cross over can be only supposed at the highest frequencies investigated, suggesting that the XG 100 at this concentration ratio is close to induce a sol-gel transition. Higher XG molar masses (XG 800 and XG 300) induce an increase in the values of G' and G'' . For both XG molar masses elastic moduli (G') is clearly higher than (G'') and do not vary with frequency.

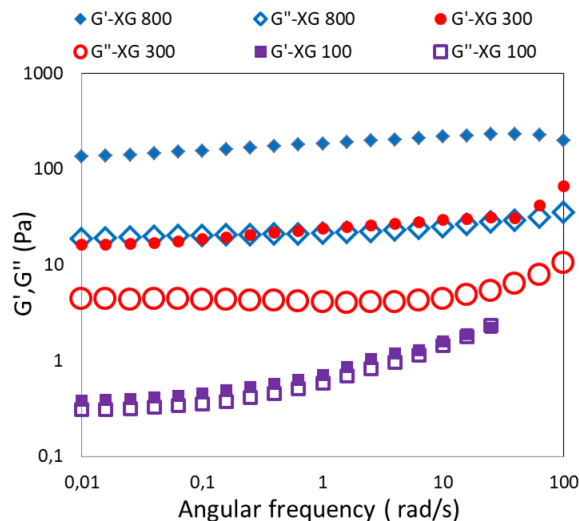


Figure 4: Effect of XG molar mass on G' and G'' moduli at different frequencies of solutions containing 15 g/L CNC + 10 g/L XG, at 20°C

The reformation capacity of the hydrogels was also investigated. Hydrogels were subjected to high shear rates. Gels broke when shear rate exceeds 100% and viscous modulus (G'') became higher than elastic (G') one (Fig. 5(a)), gels reformed instantaneously as we can see in Fig. 5(b) and recovered their initial mechanical properties in only few seconds. The interactions responsible of the gel formation are thus reversible.

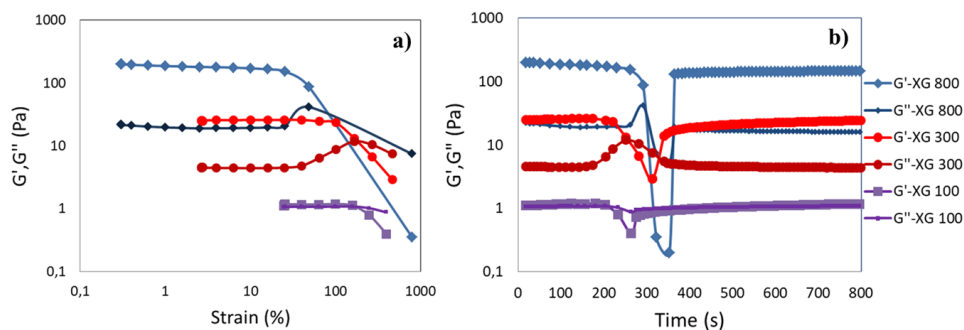


Figure 5: Variation of G' and G'' a) under strain and b) on time before and after breaking for solutions containing 15 g/L CNC + 10 g/L XG with different molar mass

4 Discussion

Tamarind XG has been fractionated by physical and enzymatic method and fractions with various molar mass have been successfully obtained. The molar masses and the monosaccharides composition were investigated. No differences were found both on the chemical structures and macromolecular features of the fractions except on the molar mass. The different behaviours found in the hydrogels properties of this study will be thus only linked to the molar mass variation.

Rheology of solutions of xyloglucans from different plant species and composition was already reported. In case of XGs with the same pattern and different molecular weight, increasing molecular weight results in the increase of the hydrodynamic volume and the radius of gyration and hence hydrodynamic volume fraction inducing an increase in viscosity [31]. Nitta *et al.* reported that tamarind XGalone does not form a gel but gelification can be obtained under specific conditions such as adding some polymers or removing substituents [32,33]. For instance, sol-gel transition of partially degalactosylated XG has been reported [34,35]. However to the best of our knowledge, there are no studies reporting the rheological behaviour of XG in presence of CNCs.

Formation of CNC based hydrogels by mixing CNC and polymers have been already reported and the mechanism of gelation can be explained by CNC depletion when the added polymers are not interacting with CNC [26,27]. When the polymers interact with CNC, the gelation might be due to either bridging between CNC or steric stabilization due to an increase of the effective hydrodynamic volume of CNC by polymer adsorption [27]. Many research studied the interactions that exist between CNC and XG. For instance the mechanism of adsorption of XG on CNCs layer has been studied in our group using quartz crystal microbalance with dissipation technique [17-19,21]. XG adsorbs instantaneously and irreversibly on cellulose nanocrystals, this adsorption is thought to be driven by an entropically and kinetically process [15,36]. Thus in the case of CNC/XG hydrogel, depletion cannot be retained as first hypothesis of the gelation mechanism. Dammak *et al.* reported that, for a high molar mass XG, saturation coverage of cotton CNC occurs at *c.a.* 300 mg XG for 1 g of CNC [18]. It was also shown that XG-CNC binding behavior was closely dependent on XG/CNC concentration ratio; at low concentration ratio, all XG is bound to CNC surface in an extended conformation forming mostly trains while at high XG/CNC ratio, XG formed loops and tails on the CNC surface. Villares *et al.* demonstrated the impact of molar mass on the XG-CNC association. They demonstrated that low molar mass xyloglucan (1.10^5 g/mol) obtained with ultrasound treatment forms an extended layer on cellulose surface, whereas high molar mass XG (10.10^5 g/mol) at the same concentration (0.1 g/L) forms accessible tails and loops [17]. Hu *et al.* proposed that adsorbing polysaccharides on CNC increased the effective volume fraction of dilute CNC dispersions by forming polymer/CNC complexes with higher hydrodynamic volume than CNC alone resulting in steric stabilization [26]. Phase diagrams of XG 800 and XG 300/CNC mixture indicate that gelation occurs at high XG/CNC ratio suggesting that the CNC surfaces are saturated. Thus, cross-linking of CNC by XG chains is unlikely and formation of XG/CNC complexes is more plausible. Consequently, gel formation through steric stabilization is the most probable mechanism. Variation of the XG molar

mass affects the adsorption process and, in an associated manner, the conformation of the XG at the CNC surface. The increase of molar mass is related to the increase of the hydrodynamic volume and the radius of gyration of the XG and hence the effective hydrodynamic volume of the XG/CNC complexes inducing an increase in viscosity then gelation. Thus higher molar mass results in higher effective hydrodynamic volume of XG/CNCs and gelation occurs at lower XG/CNC ratio (Fig. 6). Moreover., the increase in R_g and R_h increases also the probability of entanglement of coils, loops and tails of XG chains, leading to formation 3-D network. Indeed, the proportion and the size of loop and tail can thus be changed resulting in different effective hydrodynamic volume. Thus the sol-gel transitions occur at different XG/CNC ratio. The highest is molar mass, the largest is the effective hydrodynamic volume and thus the gelation occurs at lowest CNC concentration. Transient cross-links have been also proposed in the case of XG solutions to explain the rheological behaviours of XG solutions [37,38]. These short life cross-links can also exist between XG loops and tails of CNC/XG complexes. The decrease of the molar mass of XG can also reduce the number of cross-link possibility per chain. This might also explain the difference of mechanical behaviours observed between XG/CNC mixtures.

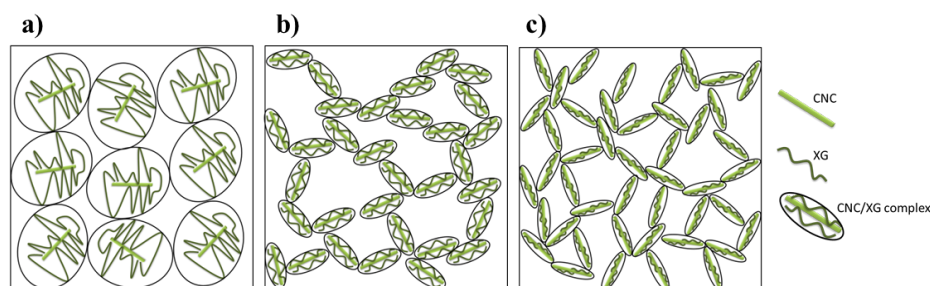


Figure 6: Schematic representation of gel formation of CNC in presence of XG at a) high, b) average and c) low molar mass

5 Conclusion

This work investigated preparation of biobased hydrogels containing exclusively CNC and XG fractions displaying different molar mass. Hydrogel formation is intimately linked to CNC and XG concentration and XG molar mass. XG/CNC gelation is due the formation of CNC/XG complexes inducing an increase of the effective hydrodynamic volume of CNC and to the interaction and entanglement between XG loops and tails. This work is the first to study the rheological properties of hydrogels containing both CNC and XG and demonstrate that it was possible to tune the rheological properties of solutions by changing XG molar mass.

References

1. Habibi, Y., Lucia, L. A., Rojas, O. J. (2010). Cellulose nanocrystals: chemistry, self-assembly, and applications. *Chemical Reviews*, 110, 3479-3500.
2. Capron, I., Rojas, O. J., Bordes, R. (2017). Behavior of nanocelluloses at interfaces. *Current Opinion in Colloid and Interface Science*, 29, 83-95.
3. De France, K. J., Hoare, T., Cranston, E. D. (2017). Review of hydrogels and aerogels containing nanocellulose. *Chemistry of Materials*, 29, 4609-4631.
4. Ling, S., Chen, W., Fan, Y., Zheng, K., Jin, K. et al. (2018). Biopolymer nanofibrils: structure, modeling, preparation, and applications. *Progress in Polymer Science*, 85, 1-56.
5. Albersheim, P. (1975). The walls of growing plant cells. *Scientific American*, 232, 81-95.
6. Hayashi, T. (1989). Xyloglucans in the primary cell wall. *Annual Review of Plant Physiology and Plant Molecular Biology*, 40, 139-168.
7. Vincken, J. P., de Keizer, A., Beldman, G., Voragen, A. (2002). Fractionation of xyloglucan fragments and their interaction with cellulose. *Plant Physiology*, 108, 1579-1585.

8. Park, Y. B., Cosgrove, D. J. (2015). Xyloglucan and its interactions with other components of the growing cell wall. *Plant and Cell Physiology*, *56*, 180-194.
9. Cosgrove, D. J. (2014). Re-constructing our models of cellulose and primary cell wall assembly. *Current Opinion in Plant Biology*, *22*, 122-131.
10. Park, Y. B., Cosgrove, D. J. (2012). A revised architecture of primary cell walls based on biomechanical changes induced by substrate-specific endoglucanases. *Plant Physiology*, *158*, 1933-1943.
11. Hayashi, T., Marsden, M. P. F., Delmer, D. P. (1987). Pea xyloglucan and cellulose. *Plant Physiology*, *83*, 384-389.
12. McCann, M. C., Roberts, K. (2017). Changes in cell wall architecture during cell elongation. *Journal of Experimental Botany*, *45*, 1683-1691.
13. Lopez, M., Marais, M., Zykwiniska, A., Ralet, M., Driguez, H. et al. (2009). Enthalpic studies of xyloglucan-cellulose interactions. *Biomacromolecules*, *11*, 1417-1428.
14. Hanus, J., Mazeau, K. (2007). The xyloglucan-cellulose assembly at the atomic scale. *Biopolymers*, *87*, 59-73.
15. Benselfelt, T., Cranston, E. D., Ondaral, S., Johansson, E., Brumer, H. et al. (2016). Adsorption of xyloglucan onto cellulose surfaces of different morphologies: an entropy-driven process. *Biomacromolecules*, *17*, 2801-2811.
16. Lopez-Sanchez, P., Schuster, E., Wang, D., Gidley, M. J., Strom, A. (2015). Diffusion of macromolecules in self-assembled cellulose/hemicellulose hydrogels. *Soft Matter*, *11*, 4002-4010.
17. Villares, A., Bizot, H., Moreau, C., Rolland-Sabaté, A., Cathala, B. (2017). Effect of xyloglucan molar mass on its assembly onto the cellulose surface and its enzymatic susceptibility. *Carbohydrate Polymers*, *157*, 1105-1112.
18. Dammak, A., Quémener, B., Bonnin, E., Alvarado, C., Bouchet, B. et al. (2015). Exploring architecture of xyloglucan cellulose nanocrystal complexes through enzyme susceptibility at different adsorption regimes. *Biomacromolecules*, *16*, 589-596.
19. Villares, A., Moreau, C., Dammak, A., Capron, I., Cathala, B. (2015). Kinetic aspects of the adsorption of xyloglucan onto cellulose nanocrystals. *Soft Matter*, *11*, 6472-6481.
20. Whitney, S. E. C., Wilson, E., Webster, J., Bacic, A., Grant Reid, J. S. et al. (2006). Effects of structural variation in xyloglucan polymers on interactions with bacterial cellulose. *American Journal of Botany*, *93*, 1402-1414.
21. Cerclier, C., Cousin, F., Bizot, H., Moreau, C., Cathala, B. (2010). Elaboration of spin-coated cellulose-xyloglucan multilayered thin films. *Langmuir*, *26*, 17248-17255.
22. Cerclier, C. V., Guyomard-Lack, A., Cousin, F., Jean, B., Bonnin, E. et al. (2013). Xyloglucan-cellulose nanocrystal multilayered films: effect of film architecture on enzymatic hydrolysis. *Biomacromolecules*, *14*, 3599-3609.
23. Kopeček, J. (2007). Hydrogel biomaterials: a smart future? *Biomaterials*, *28*, 5185-5192.
24. Chirani, N., Yahia, L., Gritsch, L., Motta, F. L., Chirani, S. et al. (2017). History and applications of hydrogels. *Journal of Biomedical Sciences*, *4*, 1-23.
25. Fan, J., Ifuku, S., Wang, M., Uetani, K., Liang, H. et al. (2018). Robust nanofibrillated cellulose hydro/aerogels from benign solution/solvent exchange treatment. *ACS Sustainable Chemistry and Engineering*, *6*, 6624-6634.
26. Hu, Z., Cranston, E. D., Ng, R., Pelton, R. (2014). Tuning cellulose nanocrystal gelation with polysaccharides and surfactants. *Langmuir*, *30*, 2684-2692.
27. Oguzlu, H., Boluk, Y. (2017). Interactions between cellulose nanocrystals and anionic and neutral polymers in aqueous solutions. *Cellulose*, *24*, 131-146.
28. Dervilly-Pinel, G., Tran, V., Saulnier, L. (2004). Investigation of the distribution of arabinose residues on the xylan backbone of water-soluble arabinoxylans from wheat flour. *Carbohydrate Polymers*, *55*, 171-177.
29. Blakeney, B. A., Harris, J. P., Henry, J. R., Stone, A. B. (1983). A simple and rapid preparation of alditol acetates for monosaccharide analysis. *Carbohydrate Research*, *113*(2), 291-299.
30. Robrnson, G. E. Y., Ross-murphy, S. B., R-morris, E. (1982). Viscosity-molecular weight relationships, intrinsic chain flexibility, and dynamic solution properties of guar galactomannan. *Carbohydrate Research*, *107*, 17-32.
31. Sims, I. M., Gane, A. M., Dunstan, D., Allan, G. C., Boger, D. V. et al. (1998). Rheological properties of xyloglucans from different plant species. *Carbohydrate Polymers*, *37*, 61-69.

32. Nitta, Y., Kim, B. S., Nishinari, K., Shirakawa, M., Yamatoya, K. et al. (2003). Synergistic gel formation of xyloglucan/gellan mixtures as studied by rheology, DSC, and circular dichroism. *Biomacromolecules*, 4, 1654-1660.
33. Nitta, Y., Nishinari, K. (2005). Gelation and gel properties of polysaccharides gellan gum and tamarind xyloglucan. *Journal of Biological Macromolecules*, 5, 47-52.
34. Brun-Graeppi, A. K. A. S., Richard, C., Bessodes, M., Scherman, D., Narita, T. et al. (2010). Study on the sol-gel transition of xyloglucan hydrogels. *Carbohydrate Polymers*, 80, 555-562.
35. Sakakibara, C. N., Sierakowski, M. R., Chassenieux, C., Nicolai, T., de Freitas, R. A. (2017). Xyloglucan gelation induced by enzymatic degalactosylation; kinetics and the effect of the molar mass. *Carbohydrate Polymers*, 174, 517-523.
36. Reid, M. S., Villalobos, M., Cranston, E. D. (2017). The role of hydrogen bonding in non-ionic polymer adsorption to cellulose nanocrystals and silica colloids. *Current Opinion in Colloid and Interface Science*, 29, 76-82.
37. De Freitas, R. A., Spier, V. C., Sierakowski, M. R., Nicolai, T., Benyahia, L. et al. (2015). Transient and quasi-permanent networks in xyloglucan solutions. *Carbohydrate Polymers*, 129, 216-223.
38. Muller, F., Jean, B., Perrin, P., Heux, L., Boué, F. et al. (2013). Mechanism of associations of neutral semiflexible biopolymers in water: the xyloglucan case reveals inherent links. *Macromolecular Chemistry and Physics*, 214, 2312-2323.